geographies

MDPI

Article

Identification of Thermal Refuges and Water Temperature Patterns in Salmonid-Bearing Subarctic Rivers of Northern Quebec

Milad Fakhari [1,*], Jasmin Raymond [1], Richard Martel [1], Stephen J. Dugdale [2] and Normand Bergeron [1]

[1] Institute National de la Recherche Scientifique, Centre Eau Terre Environnement, Quebec City, QC G1K 9A9, Canada
[2] School of Geography, University of Nottingham, Nottingham NG7 2RD, UK
* Correspondence: milad.fakhari@inrs.ca

Abstract: In summer, salmonids can experience thermal stress during extreme weather conditions. This may affect their growth and even threaten their survival. Cool water zones in rivers constitute thermal refuges, allowing fish to be more comfortable to grow and survive in extreme events. Therefore, identifying and understanding the spatiotemporal variability of discrete thermal refuges and larger scale cooling zones in rivers is of fundamental interest. This study analyzes thermal refuges as well as cooling zones in two salmonid rivers in a subarctic climate by use of thermal infrared (TIR) imagery. The two studied rivers are the Koroc and Berard Rivers, in Nunavik, Quebec, Canada. On the 17 km studied section of the Berard River, four thermal refuges and five cooling zones were detected, covering 46% of the surveyed section of the river. On the 41 km section studied for the Koroc River, 67 thermal refuges and five cooling zones were identified which represent 32% of the studied section of the river. 89% of identified thermal refuges and about 60% of cooling zones are groundwater-controlled. Continuity of permafrost and shape of the river valley were found to be the main parameters controlling the distribution of refuges and cooling zones. These data provide important insights into planning and conservation measures for the salmonid population of subarctic Nunavik rivers.

Keywords: surface water–groundwater interaction; thermal infrared imagery; thermal refuges; cooling zones; permafrost

Citation: Fakhari, M.; Raymond, J.; Martel, R.; Dugdale, S.J.; Bergeron, N. Identification of Thermal Refuges and Water Temperature Patterns in Salmonid-Bearing Subarctic Rivers of Northern Quebec. *Geographies* **2022**, 2, 528–548. https://doi.org/10.3390/geographies2030032

Academic Editors: Xu Chen and Luca Salvati

Received: 7 June 2022
Accepted: 23 August 2022
Published: 2 September 2022

1. Introduction

Rivers in northern Quebec are known for their abundance of salmonids (brook trout, Arctic char, and Atlantic salmon). Fish were an important food source for Indigenous peoples, then for the first settlers [1]. Today, fishing is still important for local communities and for revenues from sport fishing [2]. The optimal temperature range for salmonid growth varies according to species, but is generally between 7 °C and 17 °C while the lethal temperature range is 25–27 °C [3–5]. In summer, salmonids experience thermal stress in rivers as a result of higher average water temperature usually occurring on warm days with air temperature above 30 °C [6]. This affects their growth and even threatens survival. Similarly, during winter, water temperature plays an important role on spawning time and survival of buried eggs into the gravel substratum [7]. Extreme conditions in Quebec rivers are likely to occur more frequently due to climate change [8,9]. This will have a negative impact on the population of salmonids in the future, especially as certain northern species (e.g., Arctic char) are the most vulnerable with regard to thermal stress [7,10]. However, cool water zones in rivers constitute thermal refuges allowing fish to grow and to survive, even under climate extremes [11,12]. The use of thermal refuges by fish during heatwaves has been well documented [13,14]. Therefore, identifying and understanding the spatiotemporal variability of discrete thermal refuges and larger scale cooling zones in rivers is of fundamental interest to understanding fish habitat vulnerability, but still remains difficult to address at large scales.

Thermal infrared (TIR) imagery is one of the relatively low-cost solutions to evaluate large-scale surface water (SW) temperature [15]. TIR images have been used to map river water temperature [16], thermal refuges [15,17], surface water-groundwater exchange [18,19] and more specifically to monitor the thermal refuge of fish habitats [20–22]. TIR images have been used for identifying types of thermal refuges in addition to important parameters affecting them with regard to landscape variables in different rivers and watersheds [17,18,23]. However, previous studies have not examined rivers in Arctic and subarctic regions where permafrost is present. In the presence of permafrost, groundwater (GW) flow is limited [24]. Furthermore, its interaction with rivers has more complex processes that are prone to evolve due to climate change [25]. Moreover, GW-dependent refuges are most abundant and less temporally variable in rivers [15,17]. Therefore, studying processes and parameters controlling thermal refuges in rivers of high-latitude river environments is important to better anticipate their variability under climate change and thawing of permafrost.

During warm days (as targeted for this study), in a river where there is no GW seepage or if the GW seepage is constant along the river, the 'asymptotic warming paradigm' [26] indicates that river water temperature will increase from upstream to downstream since it is in contact with solar radiation for a longer period. However, in reality, a river's longitudinal temperature profile is considerably more complex, often due to the presence of cooling zones where high GW seepage occurs into the active channel. We therefore also examine these larger, diffuse GW-driven cooling zones with a view to shedding light on their controlling processes in permafrost-prone regions (as opposed to more southerly rivers, e.g., [17,26]).

The main objective of this paper is to evaluate the effect of GW-SW interaction and GW-controlled thermal refuges on river water temperature mitigation in northern rivers with the presence of permafrost. This paper therefore analyzes thermal refuges as well as cooling zones in two rivers in Nunavik, a subarctic region of Quebec, Canada (between 58° N and 59° N latitude). First, we map the distribution of thermal refuges and cooling zones using TIR imagery. We then investigate the riverscape hydromorphologic context of each refuge and cooling zone to identify critical parameters affecting water temperature, highlighting the role of GW in driving river temperature heterogeneity in a permafrost-prone region.

2. Study Area

The two studied rivers are the Koroc River and the Berard River. Both rivers are located in a subarctic climate of Nunavik, northern Quebec, Canada, and drain into Ungava Bay (Figure 1A). In previous studies, Arctic char, salmon and trout have been identified in these rivers and fishing is important for local communities [27,28].

The Berard River's source is in highlands close to the limit of the watershed of Melezes River. The river flows northwards, crosses several water bodies and lakes along its path, and ends in Ungava Bay in the northern village of Tasiujaq. The imagery of this river is for a length of 17 km downstream of Berard Lake (Figure 1B).

The Koroc River's source is located in the heights of the Torngat Mountains at the border of Labrador and Quebec, in eastern Canada. The Koroc River is located in a valley shaped by glaciers. The river runs westward and drains into the eastern shore of Ungava Bay, 18 km north of the northern village of Kangiqsualujjuaq. Thermal imagery of the Koroc River is focused on a 41 km stretch between upstream of the river delta, where the river is braided and wide, and downstream of waterfalls in the uplands, where the river flows over bedrock (Figure 1C).

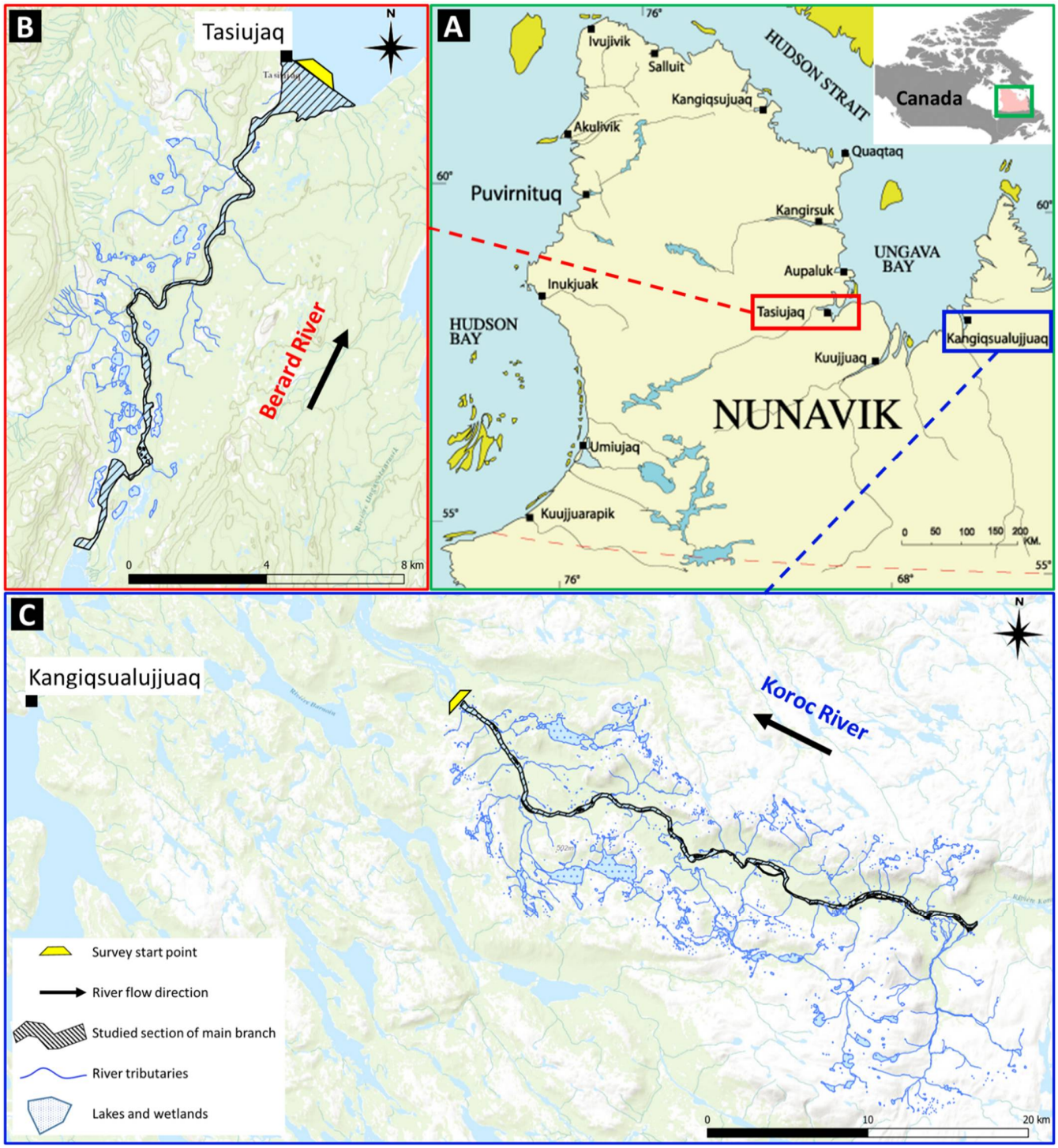

Figure 1. Location of the northern villages in Nunavik region of Quebec province (**A**), and surveyed section of the Berard River (**B**) and Koroc River (**C**).

The Berard and Koroc Rivers are located in a continental subpolar climate based on 2001 to 2010 weather data and Köppen–Geiger climate classification method [29]. The annual average temperatures in Tasiujaq and Kangiqsualujjuaq for the 1951–1980 period were −5.7 °C and −5.4 °C, respectively. For the 1981–2010 period, however, the values were −5.2 °C and −4.9 °C. Based on high emission climate scenarios, the annual average temperature is expected to become −0.3 °C and −0.2 °C for Tasiujaq and Kangiqsualujjuaq for the 2021–2050 period [30].

Average annual precipitation for the 1951–1980 period were 447 mm and 478 mm for Tasiujaq and Kangiqsualujjuaq, respectively. Based on high emission climate scenarios for the 2021–2050 period, an increase of 11% and 12% is predicted for Tasiujaq and Kangiqsualujjuaq [30]. This indicates severe trends of climate change in the Nunavik region.

The Berard River is located in the zone of discontinuous and widespread permafrost, while the Koroc River and its floodplain are in a zone of discontinuous and dispersed permafrost. However, further from the flood plain of the Koroc River, permafrost is discontinuous and widespread (Figure 2). Considering climate change trends in the region, the permafrost condition is prone to evolve [31]. The permafrost map shown in Figure 2 is based on surface temperature modeling, snow cover and other surface land metrics. This map has cells with a size of 250 m^2 [31].

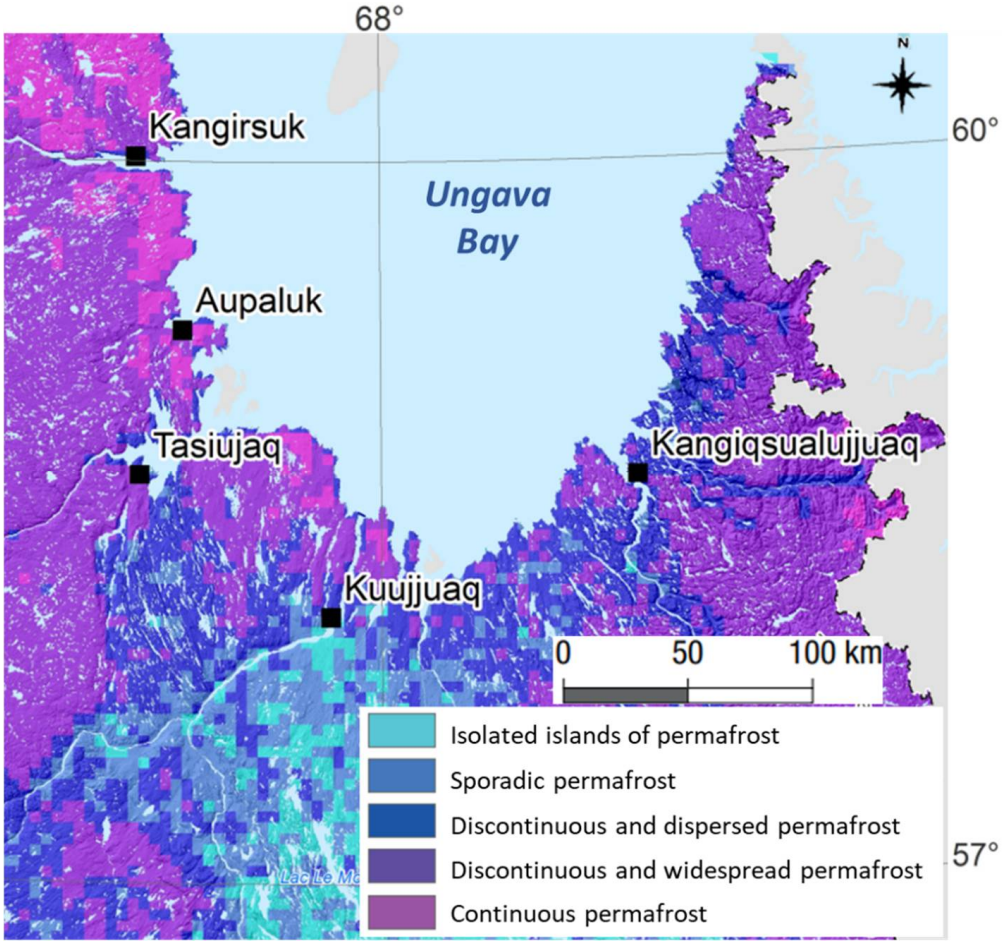

Figure 2. Permafrost map of Ungava Bay region (adapted from [31]).

The quaternary geology of both studied rivers consists of shallow sediments with a minimum thickness of 1 m. Berard River is located on glaciomarine sediments and partly on recent alluvial deposits (Figure 3A). Koroc River is located completely on alluvial deposits in the river valley and above the river valley the geology is mainly made of unconfined till and exposed bedrock (Figure 3B). The bedrock under both rivers is a mix of different types of volcanic, intrusive igneous and metamorphic rocks such as basalt, granite, marble, quartzite and gneiss belonging to Churchill Province [32].

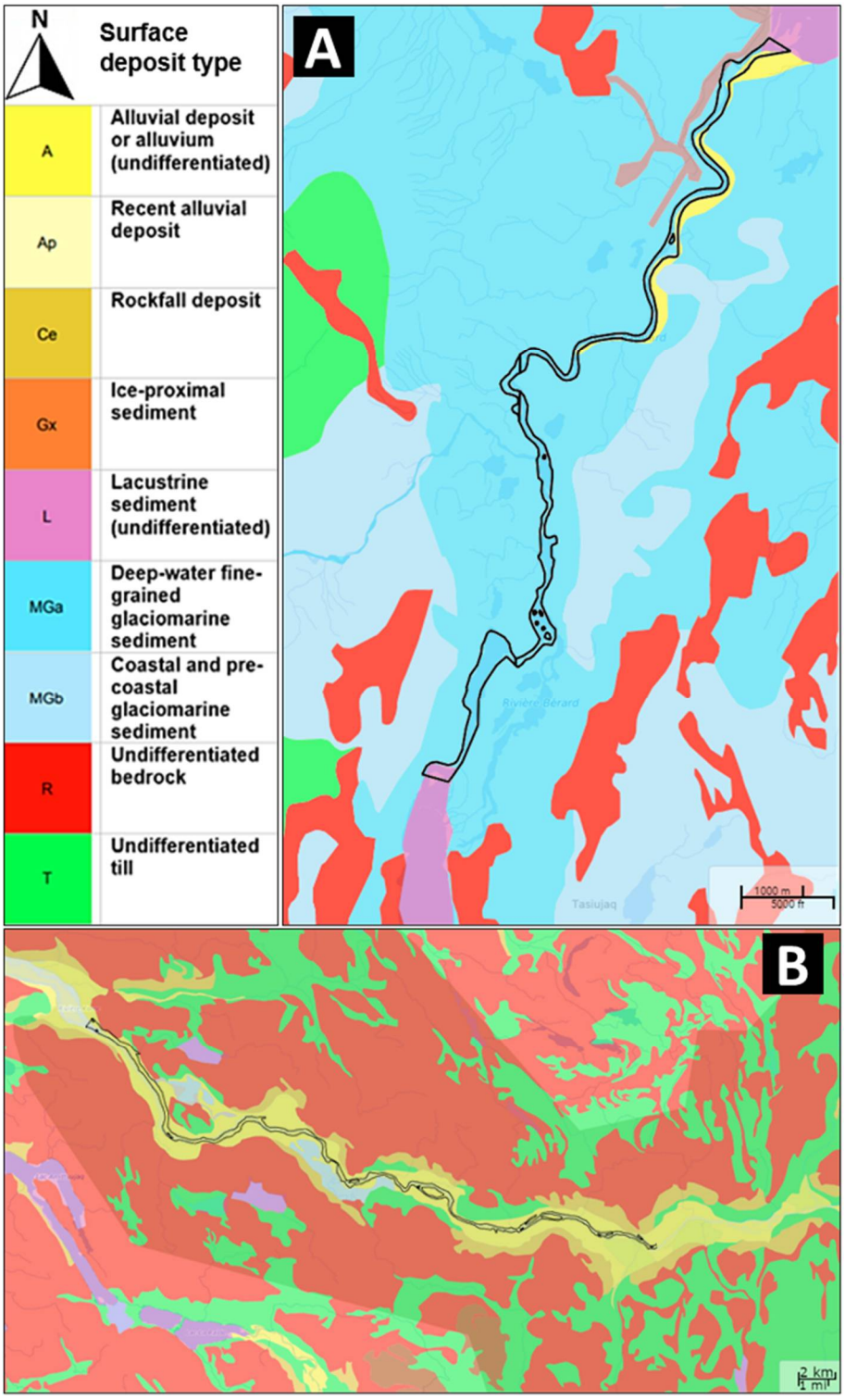

Figure 3. Surface deposits map of Berard (**A**) and Koroc (**B**) rivers (based on [32]).

3. Materials and Methods

3.1. Airborne Imagery

Airborne optical and TIR imagery of the two rivers were acquired in early August of 2019, using methods and equipment described by Dugdale et al. (2013 [15]; 2015 [17]). For optimal identification of cold water patches, the flights were conducted between 12:00 and 16:00 on a sunny day to target maximum sunlight (for optical imagery) and high river temperature (for thermal imagery), as well as low flow (based on local forecasts). Mean

flight altitude was ~750 m above ground level. Therefore, in each TIR image every pixel has a footprint of less than 0.5 × 0.5 m^2 on the ground. An image and GPS point were acquired every two seconds. Given the low groundspeed of the helicopter during survey flights, imagery has >75% overlap.

Thermal refuges were defined as a zone at least 0.5 °C cooler than the main river water temperature and an area larger than 1 m^2 [17]. Using the classification scheme in Dugdale et al. (2013) [15], the thermal refuges were divided into seven types (eight considering subgroup for wall-base channels, Table 1). Using the GPS point of each imagery and comparing the TIR and optical image pairs, we mapped the location and type of each thermal refuge. We also inspected aerial photos to confirm that thermal refuges were not false positives (e.g., shadow).

Table 1. Thermal refuge classification, showing thermal refuge types and the abbreviations used in maps (modified from [17]).

Refuge Type	Abbreviation	Description
Tributary confluence plume	T.C.P.	Cold water plume created by discharge of tributary
Lateral seep	L.S.	Bank-side cold water patch created through direct intersection of water table by river channel
Spring brook	S.B.	Cold channel emerging from floodplain depressions, springs or wetlands
Cold side channel	C.S.C.	Secondary cold channel alongside main river stem; may be ephemeral
Cold alcove	C.A.	Cold water patch at downstream end of bar; often coincides with emergence of abandoned/relict channel
Hyporheic upwelling	H.U.	Hyporheic resurgence found downstream of bars, riffles and meanders
Wall-base channel A	W.C. (A)	Cold channels formed by runoff at base of terrace (A)
Wall-base channel B	W.C. (B)	Cold channels formed by runoff on valley wall (B)

In addition to the identification of cold water zones in the river (thermal refuges), the aerial images were used to extract the temperature profile for each study river. The average river water temperature in each TIR image was calculated by averaging the temperature of three pixels in each thermal image, which were selected manually on the river central line (Figure 4, inside green). The relatively low (three) number of temperature sampling points in each image is due to: (1) anomalies at the edges of each thermal image due to vibration of the camera during flights (Figure 4, inside pink), meaning that averaging the value of the entire wetted area might introduce temperature error; (2) the high degree of overlap and position of the river channel in the center of each image meant that the inclusion of a larger number of sampling points did not change mean temperature (see the very similar temperature of all SP points in Figure 4 analysis result table).

In the next step, the mean temperature for each image was assigned with its distance from downstream, the distance of the center of each TIR image from the survey start point (yellow trapezoid shown in Figure 1). Plotting the mean water temperature of each image against its distance from downstream thus gives the temperature profile of the river.

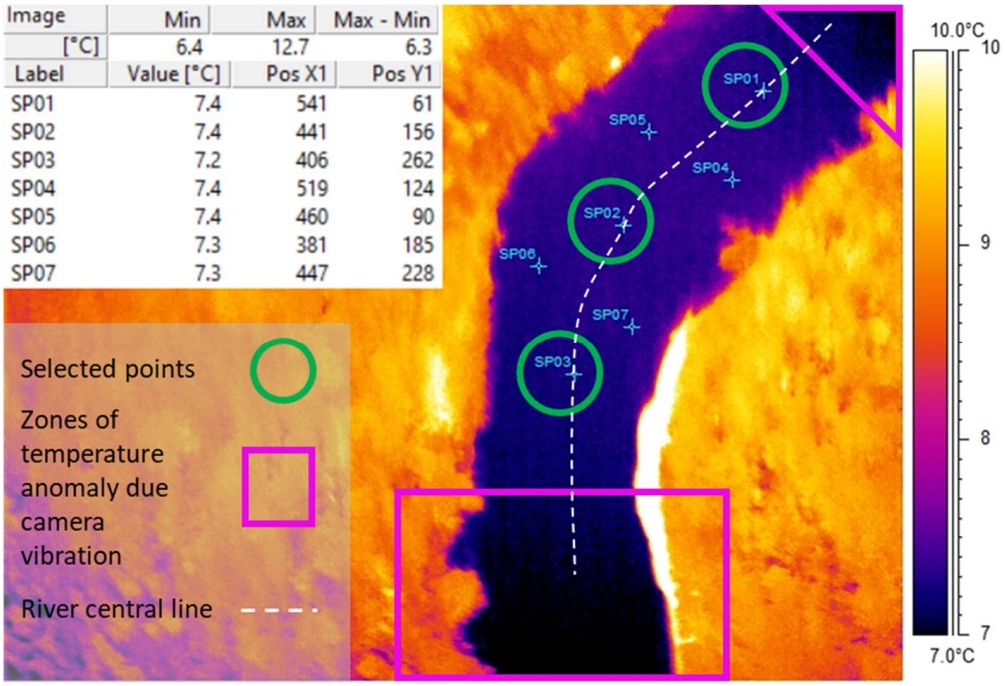

Figure 4. Example of a TIR image showing location of manually selected three points for making river water temperature average and zones of temperature anomalies caused by camera vibration.

Cooling zones were then identified using the river temperature profile. By moving downstream (value of 0 on the horizontal axis of the graph), zones that exhibited a temperature decrease >0.25 °C were identified as cooling zones. The 0.25 °C has been selected as the threshold to avoid random variation of water temperature on the graph which can be due to errors in recorded temperature by a camera in motion during the flight or the possible presence of small patches of clouds.

3.2. Links to Landscape Metrics

Different landscape metrics in three major groups mentioned below were considered for the description of the thermal refuges and cooling zones in the rivers. The landscape metrics used are those previously demonstrated to correspond to the occurrence or distribution of thermal refuges based on the work of Dugdale et al. (2015) [17]. Parameters that show a good correlation with the occurrence of thermal refuges and cooling zones can be analyzed for the identification of potential cool water, in the absence of thermal imaging.

3.2.1. Drainage Network

This group focuses on the channels and tributaries entering the main stem and their density. In the case of cooling zones, we quantified the number of tributaries in each zone. Aerial imagery and freely available water feature maps [33] were used for the identification of tributaries.

3.2.2. River Geomorphology

In this category, parameters such as river and valley width were studied. For the thermal refuge parameters at the site and for the cooling zones average of these values within the zone has been considered. In addition, river sinuosity in the cooling zone reach has been addressed (Figure 5). Measurements of width and length, are based on Open TopoMap, freely available in QGIS, with a resolution of about 30 m (1 arcsecond).

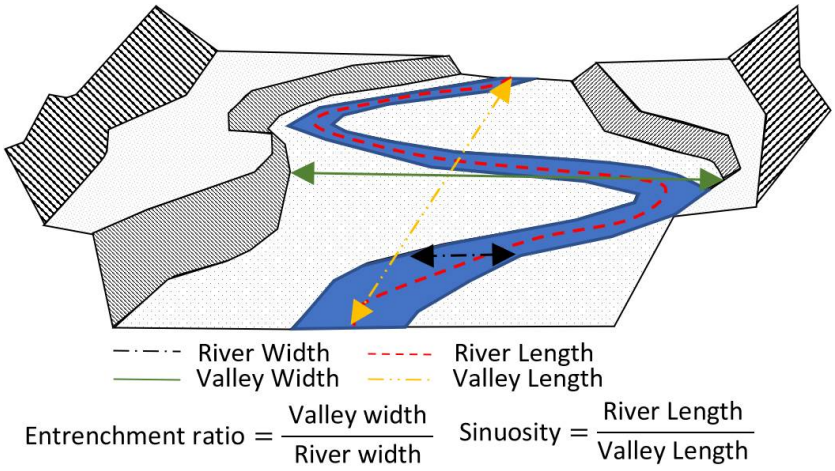

Figure 5. Schematic of river geomorphology parameters used for characterization of the cooling zones.

3.2.3. Geology and Land Cover

Vegetation and sediment type are the main factors studied in this category. Moreover, potential links to permafrost are inspected by use of available open-source maps and satellite imagery (e.g., Landsat imagery, from Google Earth imagery).

4. Results

4.1. Inventory of Thermal Heterogeneity

4.1.1. Thermal Refuges

In the studied section of the Berard River, four thermal refuges were detected: two cold side channels and two lateral seeps (Figure 6A). Considerably more thermal refuges (67) were identified in the studied section of Koroc River (Figure 6B). Considering the studied length of rivers, thermal refuge densities are 0.23 and 1.63 per kilometer for Berard and Koroc Rivers, respectively.

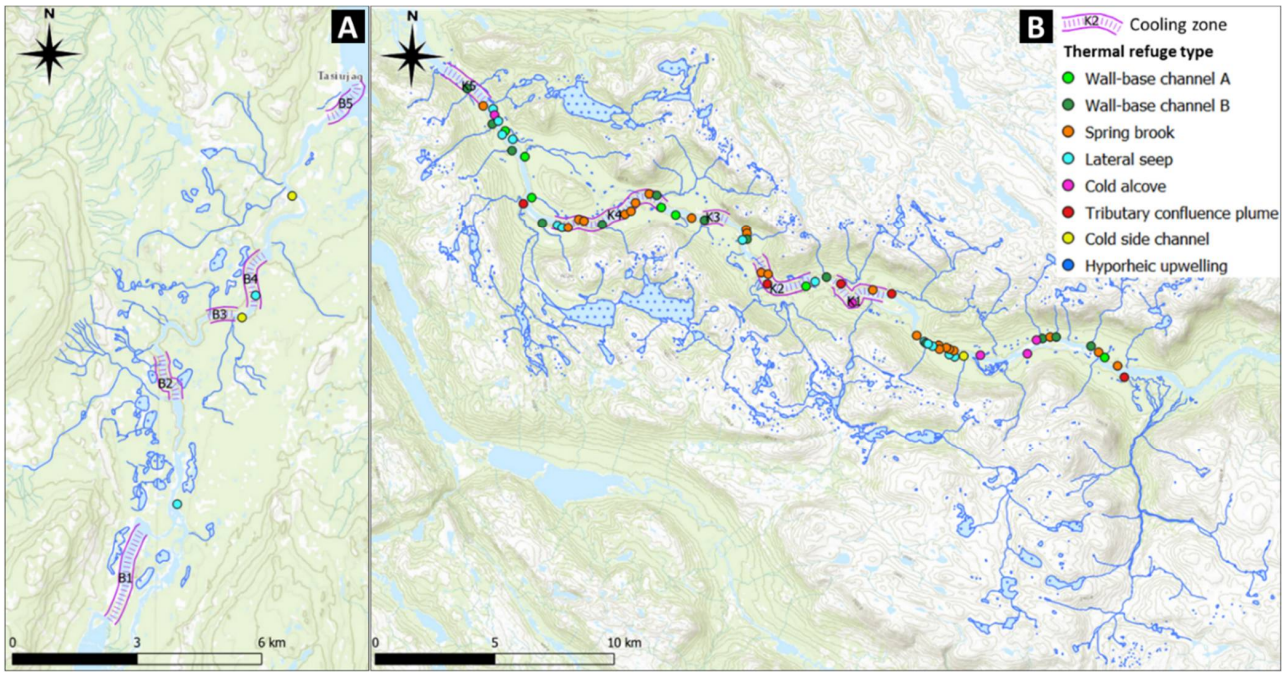

Figure 6. Location of identified thermal refuges (their type has been explained in Table 1) on studied section of Berard (**A**) and Koroc (**B**) rivers.

Sixty percent of identified thermal refuges were GW-controlled. The other 40% were tributary confluence plumes and wall-base channels, which were all detected on the Koroc River. Although GW can affect water temperature in the tributaries entering the river, tributary confluence plume and wall-base channels are not considered as GW–controlled thermal refuges. In terms of GW-controlled refuges, 49% were spring brooks, 32% lateral seeps, 11% cold alcoves, 6% cold side channels, and 2% hyporheic upwelling (Table 2).

Table 2. Identified thermal refuges.

Thermal Refuge Type	Koroc River	Berard River
Spring brook	23	
Wall-base channel	20	
Lateral seep	13	2
Cold alcove	5	
Tributary confluence plume	4	
Cold side channel	1	2
Hyporheic upwelling	1	

4.1.2. Cooling Zones

On the 17 km studied section of Berard River, five cooling zones (B1 to B5) were detected (Figure 7A), with a total length of 7.8 km, representing 46% of the surveyed section of the river. On the 41 km studied section of Koroc River, also five cooling zones (K1 to K5) were identified (Figure 7B), with a total length of 12.5 km, which is 32% of the studied section of the river. Since the width of rivers is wide relative to the height/shading of trees, the impact of shade on river temperature is negligible. The dominant cold water source (GW-SW interaction or tributaries) for each cooling zone will be investigated in the coming sections.

4.1.3. Correlation between Thermal Refuges and Cooling Zones

When comparing the location of thermal refuges and cooling zones, occurrence of thermal refuges does not guarantee the existence of cooling zones in the river, and these two phenomena might be a response to different factors. For instance, the highest temperature decrease rate for both rivers does not correspond to the highest number of thermal refuges present within a cooling zone (Table 3). However, a relationship between cooling zone length and the number of thermal refuges in the same section can be seen for the Koroc River (Figure 8A). This is not the case for Berard River. Due to the low number of identified thermal refuges on this river, only one or no thermal refuge is present in each cooling zone. Nonetheless, there is a significant correlation between the rate of water temperature decrease and the length of the cooling zone on the Berard River (Figure 8B). Moreover, since a large number of thermal refuges are wall-base channels and spring brooks in the Koroc, there is a good correlation between cooling zone length and the number of channels entering the river (Figure 8C).

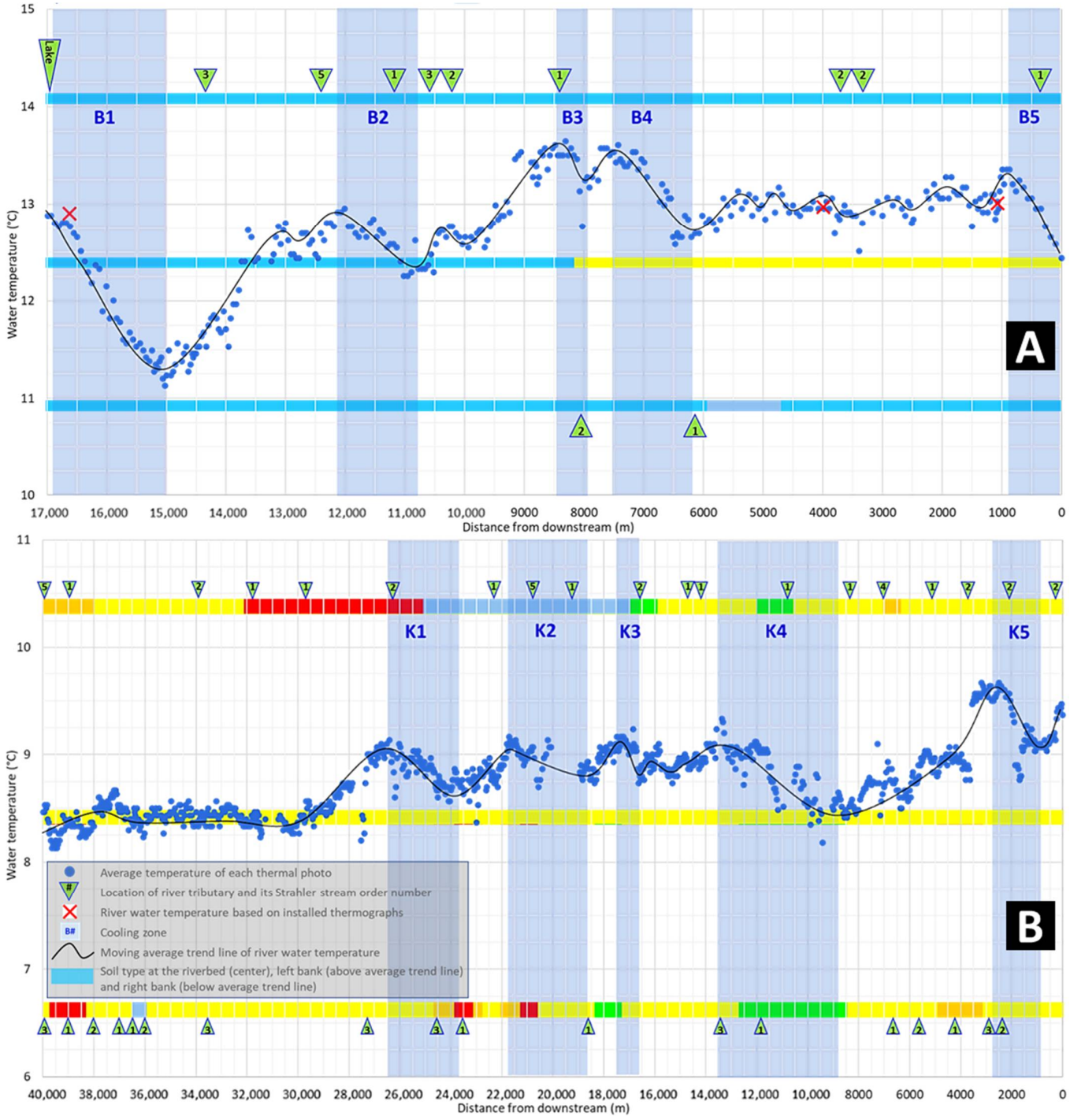

Figure 7. River water temperature profile of the Berard River (**A**) and Koroc River (**B**) with location of tributaries entering the river and surface deposit type on each side of the river (color code for soil type is the same as in Figure 3).

Table 3. Identified cooling zones' characteristics.

River	Zone	Water Temperature Decrease (°C)	Cooling Zone Length (m)	Temperature Decrease Rate (°C/km)	Valley Length (m)	Sinuosity	Average Channel Width (m)	Average Valley Width (m)	Entrenchment Ratio	Number of Thermal Refuges
Berard	B1	1.6	2363	0.68	2335	1.01	159	2154	13.57	0
	B2	0.6	1251	0.48	1100	1.14	61	1965	32.36	0
	B3	0.4	668	0.60	634	1.05	54	1526	28.26	1
	B4	0.9	1620	0.56	1433	1.13	55	2332	42.10	1
	B5	0.9	1885	0.48	1034	1.82	62	1982	32.09	0
	mean	0.9	1557.4	0.56	1307.2	1.2	78.1	1991.7	29.7	0.4
	SD	0.4	573.6	0.08	573.2	0.3	40.4	268.3	9.3	0.5
Koroc	K1	0.5	2753	0.18	2103	1.31	148	1397	9.45	3
	K2	0.3	3085	0.10	2462	1.25	236	1119	4.73	4
	K3	0.3	976	0.31	906	1.08	202	1521	7.52	1
	K4	0.7	5175	0.14	4576	1.13	201	1522	7.59	12
	K5	0.6	2253	0.27	2181	1.03	279	850	3.05	2
	mean	0.5	2512.4	0.25	2445.6	1.0	213.2	1281.9	6.5	4.4
	SD	0.2	1543.8	0.13	1191.4	0.3	43.2	261.2	2.3	3.9

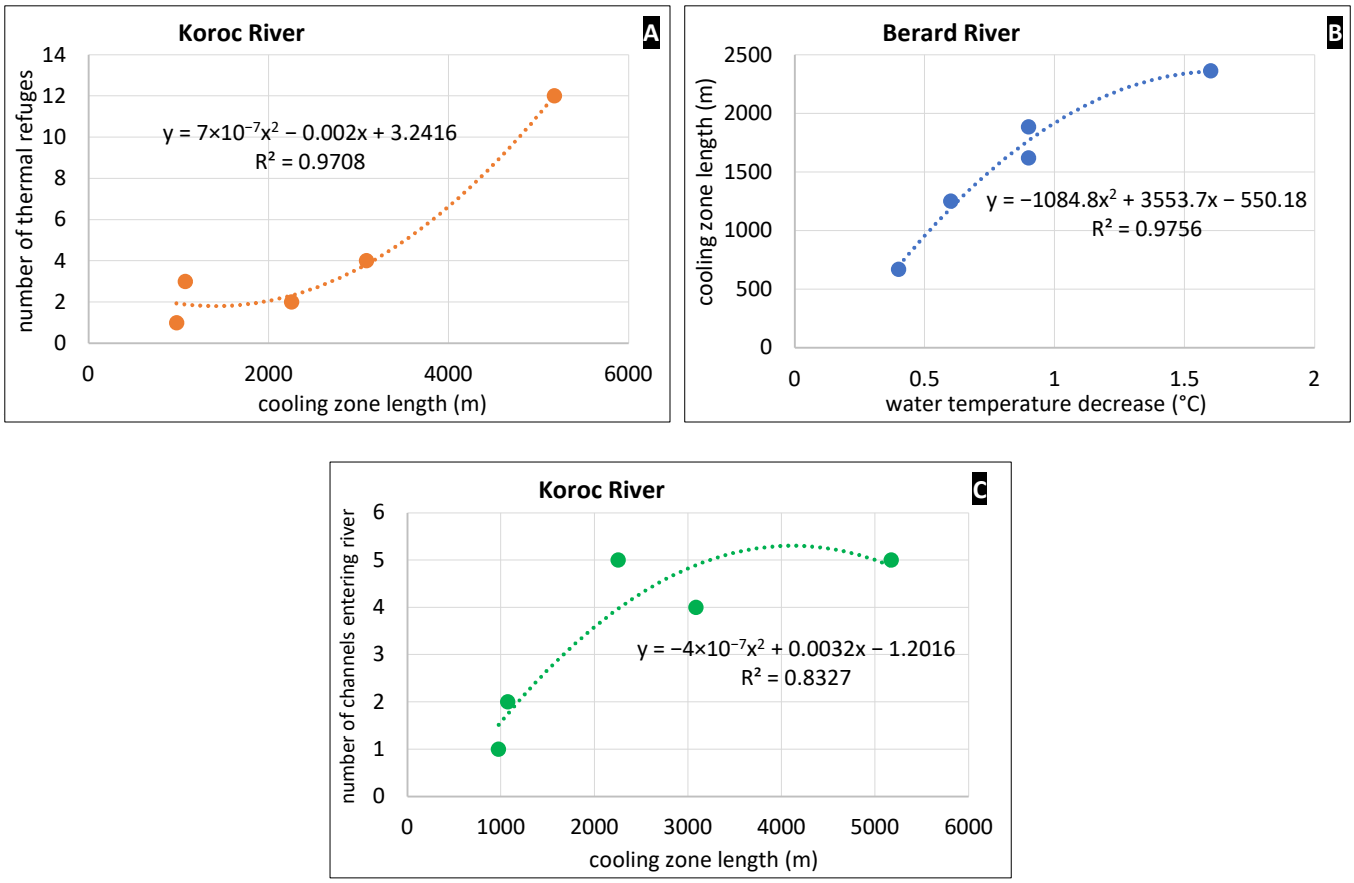

Figure 8. (**A**) Correlation between cooling zone length and number of thermal refuges in the Koroc River. (**B**) Correlation between water temperature decrease and cooling zone length in the Berard River. (**C**) Correlation between cooling zone length and number of channels entering the Koroc River.

4.2. Links to Landscape Metrics

4.2.1. Drainage Network

Tributary confluence plumes were only located on the Koroc River. The Berard River has only one significant tributary (5th order) in the studied section. Although this tributary is approximately 1 °C colder than the average main stem water temperature, it did not generate a confluence plume. This may be due to a fast mixing of cold water with the main stem river or the limited tributary discharge. Similar phenomena also occur in the Koroc River at the first cooling zone (K1), where a cold tributary enters the river without a cold

water plume observed. This suggests that for better detection of potential cold tributary confluence plume, hydraulic parameters such as the discharge and velocity of the main stem versus the tributary should be considered.

The drainage network in addition to large tributaries includes smaller channels. Smaller cold channels entering the river can form wall-base channels and spring brooks. However, differentiating between spring brooks and wall-base channels was not easy due to their morphological (but not process-based) similarity. We used drainage network analysis to aid our classification; spring brooks were considered streams formed in floodplain depressions that are only visible in the thermal or visible images but not present in the drainage network maps, whereas wall-base channels were those formed by runoff and therefore visible in the drainage network based on topographical maps. Wall-base channels are in general wider and closer to the valley walls, compared to spring brooks, which can sometimes be very narrow and only visible in thermal photos and flowing close to the river channel (Figure 9). Moreover, wall-based channels which are numerous in the studied section of the Koroc River can be classified into two types (Figure 9). The first type of channel is located within the river valley, and brings collected runoff to the river (Type A). The second type is sourced from the top of the river valley and usually connected to lakes, bringing lake outflow to the river after periods of rainfall (Type B).

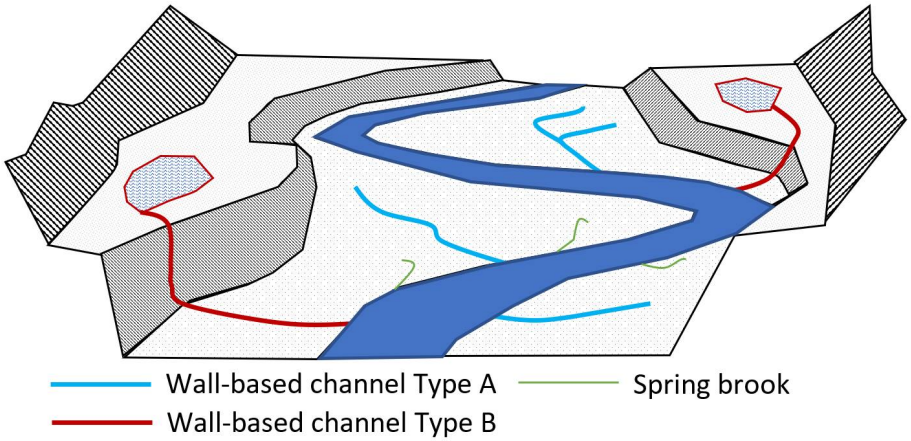

Figure 9. Schematic view of the river valley showing wall-base channels Type A and B and spring brooks.

As seen, there is a good relationship between the number of channels entering the river and the length of a cooling zone. This suggests the cooling zones are not only the result of GW influence but also SW drainage network. Looking at the maps of cooling zones and thermal refuges (Figure 6), the first two cooling zones of Koroc and Berard rivers seem to be mainly controlled by SW rather than GW. The first cooling zone in the Berard River (B1) receives cold water from an upstream lake. The second cooling zone (B2) is located after the main tributary of the Berard River having already cold water. For the Koroc River tributary confluence plumes are present within the first two cooling zones (K1 and K2). Tributary confluence plumes often have a larger effect in cooling the river compared to other (smaller) types of thermal refuges, highlighting the importance of the drainage network on the river temperature profile.

4.2.2. River Morphology

The occurrence of spring brooks and wall-base channels are related to valley shape and width. In the studied section of the Koroc River, the valley is more than 1000 m in width except for a few sections. This gives sufficient space for the development of numerous wall-base channels and spring brooks. To show the relationship of these thermal refuge types to the valley form, we calculated the entrenchment ratio by dividing valley width by river width (Figure 5). Figure 10 shows the narrowest range of entrenchment ratios

for spring brooks compared to other types followed by wall-base channel Type A. This indicates that spring brooks and wall-base channels exist in a relatively narrow range of moderate entrenchment values and are more likely to occur where valley width is on average about eight times bigger than channel width. This is different for river tributaries existing in wider valley reaches with an average entrenchment ratio of about 11 (Figure 10).

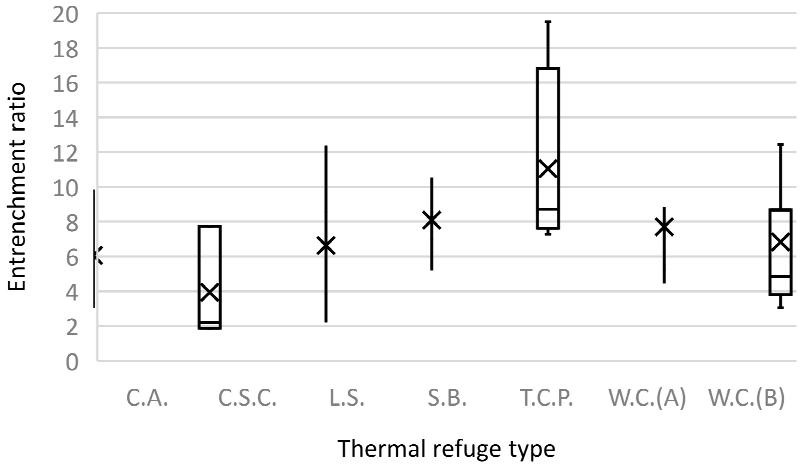

Figure 10. Entrenchment ratio range for each thermal refuge class (abbreviation of refuge classes in Table 1), showing maximum and minimum by whiskers, first and third quartile by box, median by horizontal line and mean by cross.

In the case of the cooling zones, the entrenchment ratio and sinuosity values for the Berard and Koroc Rivers vary considerably (Table 3) and moreover, are averaged over the entire zones. Therefore, a correlation cannot readily be achieved for the identification of potential cooling zones based on sinuosity or entrenchment ratio of the river.

The rate of temperature decrease for cooling zones on the Berard River is generally higher than those of the Koroc River (mean thermal gradient of -0.56 °C/km and -0.25 °C/km for Berard and Koroc Rivers, respectively). The lower average temperature decrease rate in Koroc River may be linked to its larger average width, meaning a larger effective surface area for energy exchanges (i.e., radiative/turbulent heating).

The shape of river valleys plays an important role in controlling GW-SW interaction, and can be classified as confined, semi-confined and unconfined (Figure 8 in [17]). While the Koroc River's rugged, steep valley is readily apparent from topographic maps (Figure 6, background map), the Berard River's corridor is predominantly flat. Based on the entrenchment ratio, the Koroc River is semi-confined. The upstream parts of the Berard River (upstream of B2 cooling zone and near the lake) are semi-confined, the downstream section is principally unconfined.

This difference in entrenchment ratio also explains the high number of thermal refuges in the Koroc River in comparison to the Berard. In the Koroc, local GW flow has an influential role in driving refuge distribution, whereas in the Berard River, the river valley is flatter, therefore, thermal refuges which are derived by local GW flow are limited.

4.2.3. Geology and Land Cover

The main vegetation cover of the Koroc River valley is a coniferous forest in four subgroups of tree cover. However, on top of the river valley, the vegetation cover has lower density and more exposed bedrock (Figure 11A). Surface deposits under the Koroc River and within the river valley consist mainly of alluvium (A), although in some zones of the river valley, costal and pre-costal glaciomarine sediments (MGa) as well as rockfall deposits (Ce) are also present. The sediments in the river valley are more permeable than other surface deposits such as till (T) and bedrock (R) present on top of the river valley (Figure 11B).

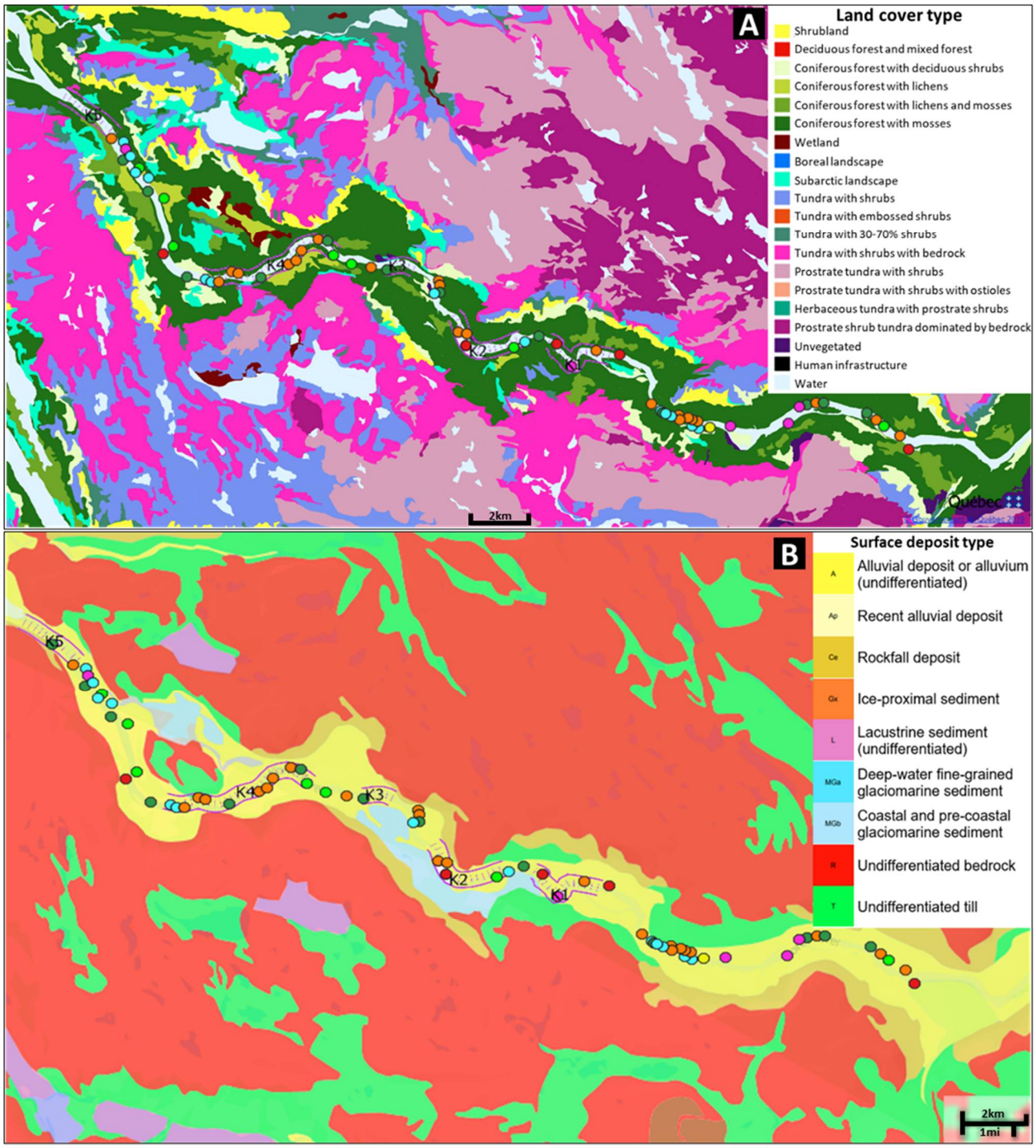

Figure 11. Land cover ((**A**), based on [34]) and surface deposits ((**B**), based on [32]) of the Koroc River study area (legend for thermal refuges and cooling zones same as in Figure 6).

At the studied section of the Berard River, the landcover is predominantly composed of shrublands with a mix of wetlands and tundra with shrubs (Figure 12A). Surface deposits below and next to the Berard River are mainly deep-water fine-grained glaciomarine sediments. Based on available morpho-sedimentological maps, alluvium is only present in the downstream section of the Berard River (Figure 12B). The difference in scale of the Berard River compared to the Koroc River can suggest a lower potential for sedimentation and shallower alluvium for the Berard River.

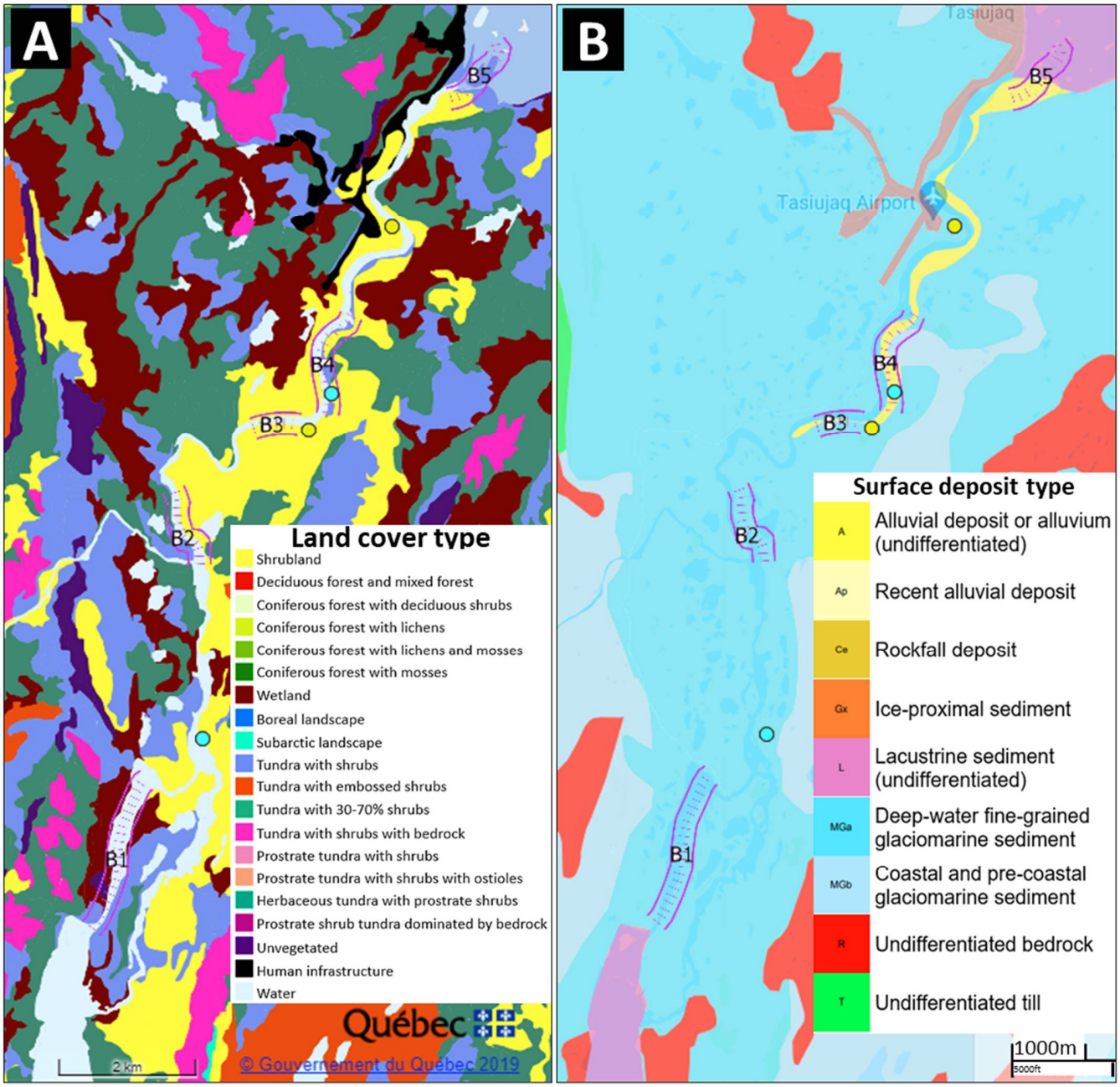

Figure 12. Land cover ((**A**), based on [34]) and surface deposits ((**B**), based on [32]) of the Berard River study area (legend for thermal refuges and cooling zones same as in Figure 6).

The presence of a specific soil or vegetation type cannot be used to pinpoint the existence of thermal refuge. In the case of the Koroc River, the entire studied section of the river is on alluvium and surrounded by coniferous forest. For the Berard River case, all thermal refuges are located in land-use comprising shrubland vegetation; three of them are on alluvium and one on glaciomarine deposits. The difference in the number of thermal refuges between the two studied rivers indicates that a higher density of vegetation and the presence of thicker permeable materials may be linked to higher thermal refuge density.

While we hoped to assess linkages between permafrost coverage and the location of thermal refuges, the resolution of permafrost maps (Figure 2) for the region is insufficient for establishing any such relationships. Based on Figure 2, both studied rivers are located entirely on one type of permafrost, potentially limiting further analysis. However, other available permafrost maps suggest discontinuous permafrost closer to Ungava Bay for

the Koroc River (Figure 13). This dataset indicates that all cooling zones and more than 60% of thermal refuges on the Koroc River are located on downstream sections where discontinuous permafrost is present. This suggests discontinuity of permafrost may favor higher GW-SW interaction and the existence of abundant thermal refuges.

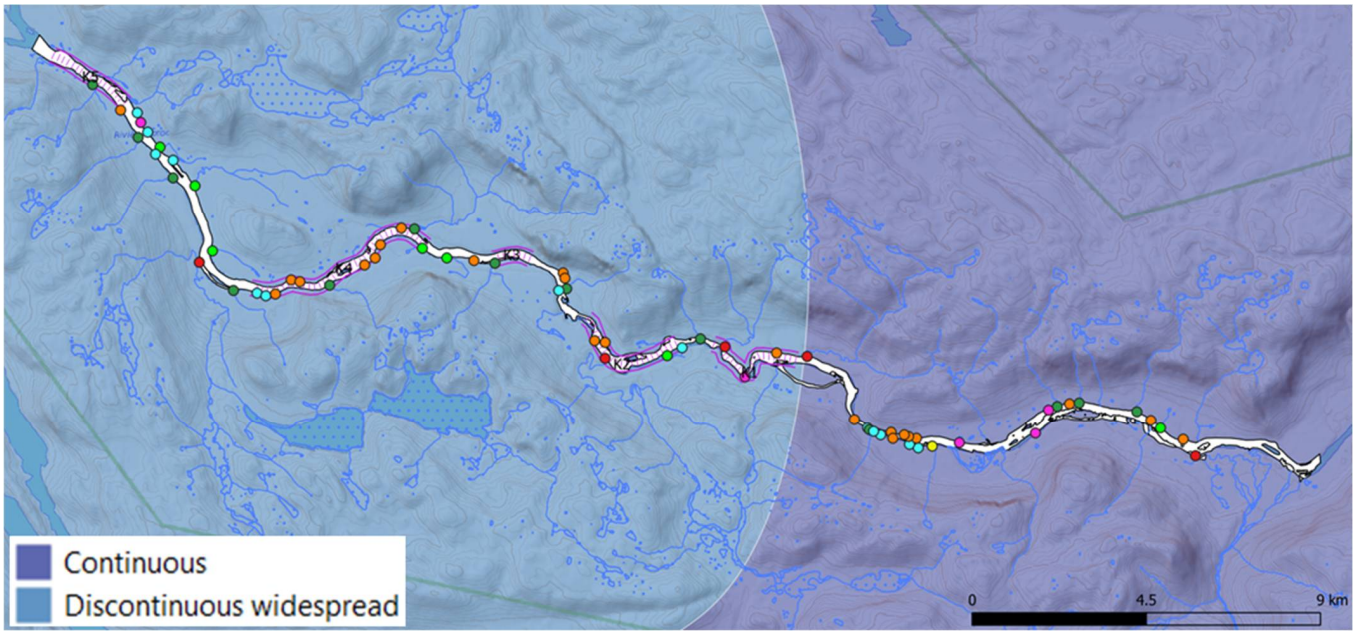

Figure 13. Location of Koroc River thermal refuges and cooling zones on permafrost continuity map (adapted from [35]).

Aerial and satellite imagery can further be used for permafrost mapping and monitoring [36], with a view to examining links to the distribution of thermal refuges or riverine cooling zones. The presence of thermokarst lakes around the Berard and Koroc Rivers suggests the existence of permafrost near these two rivers (Figure 14). A thermokarst lake forms when land subsidence caused by a thaw of permafrost is filled by water [37]. The absence of such lakes inside the Koroc River valley is also an indicator of the absence of continuous permafrost. Both increase [38] or decrease [39] in the size of thermokarst lakes show degradation of permafrost. The decrease or increase in size depend on different factors and thawing stage of permafrost, and have been used in remote sensing studies to monitor permafrost condition in arctic regions. Comparing Figure 14, a decrease in the size of the lake south of the Tasiujaq airport can be observed suggesting internal drainage of the lake to the Berard River, through degradation of shallow permafrost. Regarding Koroc River obvious changes in the size of lakes are not observed in available satellite images, which can suggest a more stable condition for permafrost. The stability of permafrost near Koroc River can be due to the absence of significant sedimentary deposits at the top of the river valley which sits on the bedrock. Another thermokarst landform, beaded streams, forms when thermokarst lakes connect and form a river with pools and riffles [40] (Figure 14). These types of streams are regularly found on the plateau outside of the Koroc River's valley. The Berard River itself can be considered as a beaded stream. Especially upstream of its main tributary, there are parts of the river that are wider and deeper and form pools. Since a pool section of a river is deeper, it is more probable that permafrost is degraded and the river connects to the aquifer. However, under shallow riffle sections of river permafrost can be present. These observations (based on satellite imagery) again suggest better continuity of permafrost nearer the Berard River and less potential for GW-SW interaction compared to Koroc River.

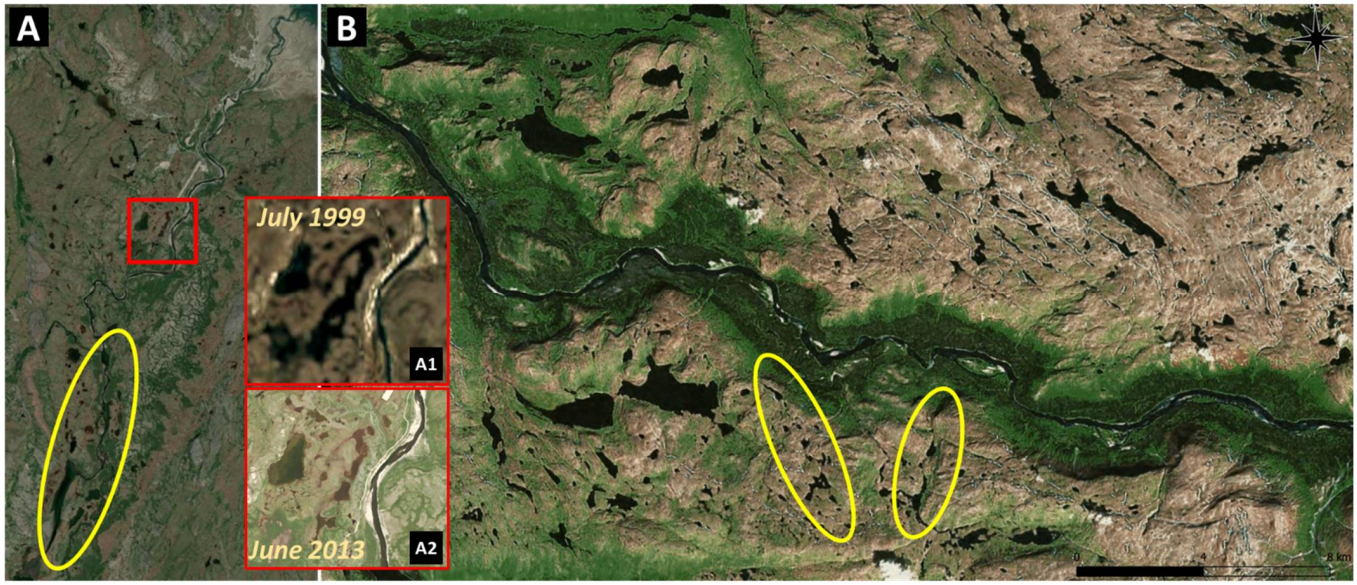

Figure 14. Satellite imagery (June 2013 Google earth Landsat images) of Berard (**A**) and Koroc (**B**) Rivers showing presence of thermokarst lakes and beaded streams (examples inside yellow circles).

5. Discussion

The difference in the number of identified thermal refuges between Koroc and Berard rivers can be related to a range of hydromorphic, environmental and geologic characteristics, such as valley confinement, geology, vegetation cover and permafrost condition. The semi-confined shape of Koroc River valley explains both the abundance of wall-base channels relating to runoff processes within/on the valley, and also spring brook refuges where contact between valley wall and floor can drive GW seepage (e.g., [17]). Due to less permeable surface deposits and less vegetated land cover, the valley tops are prone to runoff. On the other hand, in the river valley the presence of more permeable materials and higher vegetation cover favor GW infiltration/seepage and GW-SW interconnection (e.g., [41]). This, in combination with less continuous permafrost around the Koroc River compared to the Berard River, can explain the large difference in the number and density of thermal refuges between the two rivers (i.e., higher density in the Koroc River).

Machine learning and remote sensing combinations have been used to identify the location of thermal refuges and GW-SW interaction zones in numerous rivers (e.g., [17,42–44]). In these studies, key landscape parameters (e.g., channel confinement, location of dry valleys) have been noted as potential predictors for the location of thermal refuges. In our paper, such relationships have not been achieved for either the Koroc and Berard Rivers because: (1) the two rivers have different characteristics (valley shape, size, etc.), (2) a reliable dataset to build and train such models (length of studied river sections and the number of identified thermal refuges and cooling zones) has not yet been achieved, and (3) detailed data such as LiDAR topographic maps or permafrost map from geophysical field measurements are not available. Nevertheless, the effect of the number of channels (i.e., tributary valley distance) and entrenchment ratio on river water temperature is apparent for both rivers (similar to findings by Dugdale et al., 2015 [17]). Our study also shows that the use of TIR aerial images is a reliable way to detect cool zones in subarctic rivers. TIR images show good results for the identification of spring brook and low-order wall-base channels that cannot be identified from lower resolution DEMs that are typical in such data-sparse regions. The large number of spring brooks and wall-base channels suggested that studying the temperature of channels entering the river and identifying possible locations where GW-fed channels can appear is important when it comes to the identification of potential spawning and juvenile salmonid habitats (e.g., [43,45]) in subarctic rivers.

The available permafrost maps were developed at a regional scale using a model and are thus unsuited to analyze linkages to individual thermal refuges or cooling zones in the studied rivers. The use of airborne GPR (ground-penetrating radar) alongside with TIR imagery could be a possible solution to establish such a correlation between thermal refuges and the existence of permafrost or depth of active layer where discontinuous permafrost exists (e.g., [46,47]). Nevertheless, the results from satellite imagery and results from the permafrost map for the Koroc River study site (Figure 13) suggest a possible linkage to the continuity of permafrost.

The role of permafrost in GW-SW interaction for northern rivers is well known [24,25,35]. Open taliks can be formed under surface water bodies where lakes or rivers are larger and deeper, such as the Koroc River. A talik refers to soil that is unfrozen throughout the year and normally present under thermokarst lakes and rivers. Open taliks connect the subpermafrost aquifer and the river (Figure 15); therefore, the presence of GW-based cooling zones is probable in these areas. In the case of smaller rivers like the Berard River, only closed taliks are formed; therefore, river can only interact with suprapermafrost aquifer (Figure 15). The suprapermafrost is less thick, meaning that the GW flow is limited, but since it flows over permafrost, water temperature is generally colder. GW flow over permafrost can therefore explain existence of cold thermal refuges within cooling zones or in general in arctic rivers of this study that have generally cooler water temperature compared to rivers in the south.

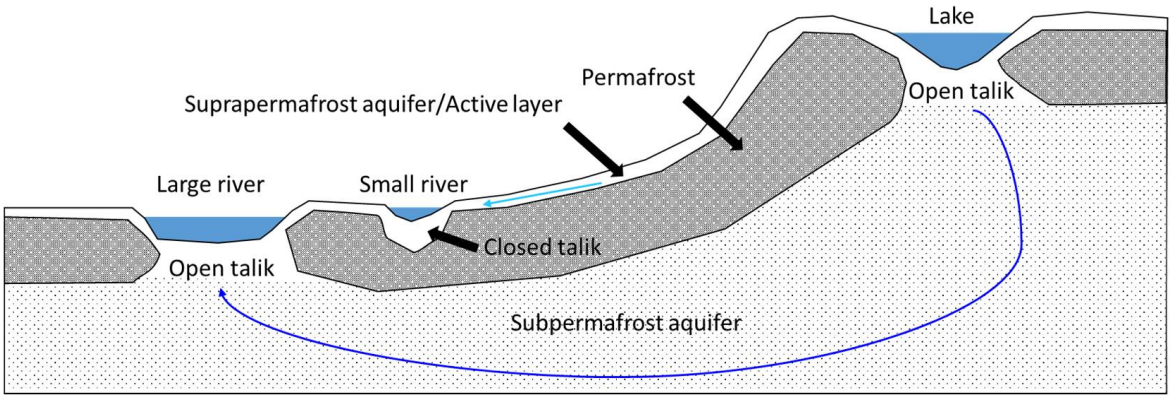

Figure 15. Schematic cross-section showing the different types of aquifers and groundwater flow paths in presence of permafrost (adapted from [35]).

Changes in the size of thermokarst lakes near the Berard River can be an indication of evolving GW-SW interaction caused by the thaw of permafrost. Considering the changing climate of northern Quebec and the predicted thaw of the permafrost [31], the GW influence on the thermal budget of rivers in arctic and subarctic regions may become more important in the future. It is possible that more GW thermal refuges will appear in the future, potentially offsetting the climatic warming of surface waters because the thaw of permafrost changes GW flow patterns. However, this is far from certain, and the future evolution of river temperature patterns in the region is currently unknown. Nevertheless, even if increased groundwater contributions may offset other climate-forced river temperature warming (and thus in-stream heat-stress events), any river temperature change will likely change fish migration patterns (since the spawning and upstream migration cues are dependent on water temperature [7]), with potential other serious consequences for northern salmonid populations.

6. Conclusions

In total, 71 thermal refuges over 58 km studied reaches of the Koroc and Berard Rivers, Nunavik, Quebec, were identified. The majority of identified thermal refuges are GW-controlled, but non-GW-controlled thermal refuges were present in substantial numbers (i.e., wall-base channels and tributary confluence plumes). Five cooling zones on each river

were also observed. 40% of observed cooling zones are under influence of SW inlets either from upstream lakes or tributaries. For the other 60%, the absence of such SW intakes suggests that the cooling zone is the effect of GW-SW interaction. Therefore, it can be confirmed that GW plays an important role in river temperature mitigation.

Due to the small case study size and differences between the two studied rivers, no parameter within the three groups of landscape metrics showed a direct connection to the existence of thermal refuges or cooling zones. However, similar to previous studies, river entrenchment ratio and shape of the river valley were nonetheless linked to the occurrence of thermal refuges. Further investigation specific to northern latitude rivers is therefore needed to better identify important parameters in driving the occurrence of thermal refuges.

Permafrost continuity plays an important role in the degree of GW-SW interaction for northern rivers. The permafrost for the Berard River is more continuous than the Koroc River and as a result, fewer thermal refuges are present. Based on previous studies, GW-controlled thermal refuges were shown to be less temporally variable [15]. However, the same cannot be confirmed for northern rivers. Permafrost can partly or completely freeze and restrict GW flow. Therefore, thermal refuges driven from suprapermafrost aquifer can vary seasonally. Moreover, regarding a longer time scale, satellite imagery analysis near Berard River suggests that changes in the permafrost condition for the region have started. Thaw of permafrost will lead to higher GW recharge, thus potentially to higher GW flow. Here, the increased outflow of these lakes to the nearby river is expected. Therefore, GW flow will have more influence on river water temperature, and the number of GW-controlled thermal refuges may increase in the future. The speed of changes depends on other features such as the sediment and bedrock types. Zones with potentially continuous permafrost for the Koroc River are on bedrock and, thus, changes in the GW flow system are less visible and may appear later. Future implementation of such studies will better show temporal variation of thermal refuges and GW influence on river thermal budget. This study has helped to better understand GW-SW interaction on river water temperature for future application in fish habitat monitoring and river management of northern Quebec.

Author Contributions: Conceptualization, M.F., J.R. and R.M.; methodology, S.J.D. and N.B.; formal analysis, M.F.; data curation, M.F.; writing—original draft preparation, M.F.; writing—review and editing, M.F., J.R., R.M., S.J.D. and N.B.; visualization, M.F. All authors have read and agreed to the published version of the manuscript.

Funding: This project was undertaken with the financial support of the Government of Canada.

Data Availability Statement: The data are not publicly available since, data was obtained from indijinous communities' category 1 and 2 lands and are available from the corresponding author with the permission of northern village office and land holding of Tasiujaq and Kangiqsualujjuaq and Kuururjuaq national park office.

Conflicts of Interest: The authors declare no conflict of interest.

References

1. April, J.; Arvisais, M. *Atlantic Salmon Management Plan 2016–2026. Ministère des Forêts, de la Faune et des Parcs, Direction Générale de L'expertise sur la Faune et ses Habitats*; Direction de la Faune Aquatique: Quebec City, QC, Canada, 2016; p. 40.
2. Poesch, M.S.; Chavarie, L.; Chu, C.; Pandit, S.N.; Tonn, W. Climate change impacts on freshwater fishes: A Patagonian perspective. *Fisheries* **2016**, *41*, 385–391. [CrossRef]
3. Finstad, A.; Jonsson, B. Effect of incubation temperature on growth performance in Atlantic salmon. *Mar. Ecol. Prog. Ser.* **2012**, *454*, 75–82. [CrossRef]
4. Nyanti, L.; Soo, C.L.; Ahmad-Tarmizi, N.N.; Ling, T.Y.; Sim, S.F.; Grinang, J.; Ganyai, T. Effects of water temperature, dissolved oxygen and total suspended solids on juvenile barbonymus schwanenfeldii (Bleeker, 1854) and Oreochromis Niloticus (Linnaeus, 1758). *Aquac. Aquar. Conserv. Legis.* **2018**, *11*, 394–406.
5. Jensen, A.J.; Johnsen, B.O.; Saksgård, L. Temperature requirements in *Atlantic salmon* (*Salmo salar*), *Brown trout* (*Salmon trutta*), and *Arctic char* (*Salvelinus alpinus*) from hatching to initial feeding compared with geographic distribution. *Can. J. Fish. Aquat. Sci.* **1989**, *46*, 786–789. [CrossRef]

6. Gunn, J.; Snucins, E. Brook charr mortalities during extreme temperature events in Sutton River, Hudson Bay Lowlands, Canada. *Hydrobiologia* **2010**, *650*, 79–84. [CrossRef]
7. Jonsson, B.; Jonsson, N. A review of the likely effects of climate change on anadromous Atlantic salmon Salmo salar and brown trout Salmo trutta, with particular reference to water temperature and flow. *J. Fish Biol.* **2009**, *75*, 2381–2447. [CrossRef]
8. Palko, K.G.; Lemmen, D.S. *Climate Risks and Adaptation Practices for the Canadian Transportation Sector 2016*; Transport Canada: Ottawa, ON, Canada, 2017; pp. 182–216.
9. Power, G.; Brown, R.S.; Imhof, J.G. Groundwater and fish—Insights from northern North America. *Hydrol. Process.* **1999**, *13*, 401–422. [CrossRef]
10. Baroudy, E.; Elliott, J.M. The critical thermal limits for juvenile Arctic charr Salvelinus alpinus. *J. Fish Biol.* **1994**, *45*, 1041–1053. [CrossRef]
11. Lorenz, J.M.; Filer, J.H. Spawning Habitat and Redd Characteristics of Sockeye Salmon in the Glacial Taku River, British Columbia and Alaska. *Trans. Am. Fish. Soc.* **1989**, *118*, 495–502. [CrossRef]
12. Geist, D.R.; Dauble, D.D. Redd site selection and spawning habitat use by fall chinook salmon: The importance of geomorphic features in large rivers. *Environ. Manag.* **1998**, *22*, 655–669. [CrossRef]
13. Breau, C.; Cunjak, R.A.; Bremset, G. Age-specific aggregation of wild juvenile Atlantic salmon Salmo salar at cool water sources during high temperature events. *J. Fish Biol.* **2007**, *71*, 1179–1191. [CrossRef]
14. Berman, C.H.; Quinn, T.P. Behavioural thermoregulation and homing by spring chinook salmon, Oncorhynchus tshawytscha (Walbaum), in the Yakima River. *J. Fish Biol.* **1991**, *39*, 301–312. [CrossRef]
15. Dugdale, S.J.; Bergeron, N.E.; St-Hilaire, A. Temporal variability of thermal refuges and water temperature patterns in an Atlantic salmon river. *Remote Sens. Environ.* **2013**, *136*, 358–373. [CrossRef]
16. Torgersen, C.E.; Faux, R.N.; A McIntosh, B.; Poage, N.J.; Norton, D.J. Airborne thermal remote sensing for water temperature assessment in rivers and streams. *Remote Sens. Environ.* **2001**, *76*, 386–398. [CrossRef]
17. Dugdale, S.J.; Bergeron, N.E.; St-Hilaire, A. Spatial distribution of thermal refuges analysed in relation to riverscape hydromorphology using airborne thermal infrared imagery. *Remote Sens. Environ.* **2015**, *160*, 43–55. [CrossRef]
18. Casas-Mulet, R.; Pander, J.; Ryu, D.; Stewardson, M.J.; Geist, J. Unmanned Aerial Vehicle (UAV)-Based Thermal Infra-Red (TIR) and Optical Imagery Reveals Multi-Spatial Scale Controls of Cold-Water Areas Over a Groundwater-Dominated Riverscape. *Front. Environ. Sci.* **2020**, *8*, 64. [CrossRef]
19. Dole-Olivier, M.-J.; Wawzyniak, V.; Châtelliers, M.C.D.; Marmonier, P. Do thermal infrared (TIR) remote sensing and direct hyporheic measurements (DHM) similarly detect river-groundwater exchanges? Study along a 40 km-section of the Ain River (France). *Sci. Total Environ.* **2018**, *646*, 1097–1110. [CrossRef]
20. Bergeron, N.; Carbonneau, P.E. Geosalar: Innovative Remote Sensing Methods for Spatially Continuous Mapping of Fluvial Habitat at Riverscape Scale. In *Fluvial Remote Sensing for Science and Management*, 1st ed.; Carbonneau, P.E., Piegay, H., Eds.; John Wiley and Sons: Chichester, UK, 2012; pp. 193–213.
21. Dugdale, S.J.; Franssen, J.; Corey, E.; Bergeron, N.E.; Lapointe, M.; Cunjak, R.A. Main stem movement of Atlantic salmon parr in response to high river temperature. *Ecol. Freshw. Fish* **2016**, *25*, 429–445. [CrossRef]
22. Thomas, T.; Council, F.B.; Willms, T.; Bio, R.P.; Whitworth, G. *Mapping of Critical Summer Thermal Refuge Habitats for Chinook Salmon, Coho salmon, Steelhead and Bull trout in the Nicola River Watershed—2016*; Fraser Basin Council: Kamloops, BC, Canada, 2017.
23. Monk, W.; Wilbur, N.M.; Curry, R.A.; Gagnon, R.; Faux, R.N. Linking landscape variables to cold water refugia in rivers. *J. Environ. Manag.* **2013**, *118*, 170–176. [CrossRef]
24. Liao, C.; Zhuang, Q. Quantifying the Role of Permafrost Distribution in Groundwater and Surface Water Interactions Using a Three-Dimensional Hydrological Model. *Arctic. Antarct. Alp. Res.* **2017**, *49*, 81–100. [CrossRef]
25. Lamontagne-Hallé, P.; McKenzie, J.M.; Kurylyk, B.L.; Molson, J.; Lyon, L.N. Guidelines for cold-regions groundwater numerical modeling. *WIREs Water* **2020**, *7*, e1467. [CrossRef]
26. Fullerton, A.H.; Torgersen, C.E.; Lawler, J.J.; Faux, R.N.; Steel, E.A.; Beechie, T.J.; Ebersole, J.L.; Leibowitz, S.G. Rethinking the longitudinal stream temperature paradigm: Region-wide comparison of thermal infrared imagery reveals unexpected complexity of river temperatures. *Hydrol. Processes* **2015**, *29*, 4719–4737. [CrossRef]
27. Mainguy, J.; Beaupré, L. Établissement d'un état de référence pour la population d'omble chevalier de la rivière Bérard à Tasiujaq. In *Report for Ministère des Forêts, de la Faune et des Parcs, Direction de L'expertise sur la Faune Aquatique et Direction de la Gestion de la Faune du Nord-du-Quebec*; Ministère des Forêts, de la Faune et des Parcs (MFFP): Quebec City, QC, Canada, 2019; p. 29.
28. Kativik Regional Government. *Kuururjuaq Park Project (Monts-Torngat-et-Rivière Koroc), Status Report*; Ministère des Forêts, de la Faune et des Parcs (MFFP): Quebec City, QC, Canada, 2005.
29. Gouvernement du Quebec. Normales Climatiques 1981–2010. Available online: http://www.environnement.gouv.qc.ca/climat/normales/climat-qc.htm (accessed on 1 September 2021).
30. ClimateData.ca. Environment and Climate Change Canada Data Servers End-Use Licence. Available online: https://eccc-msc.github.io/open-data/licence/readme_en/ (accessed on 1 September 2021).
31. L'Hérault, E.; Allard, M. *Production de la 2ième Approximation de la Carte de Pergélisol du Quebec en Fonction des Paramètres Géomorphologiques, Écologiques, et des Processus Physiques Liés au Climat*; Quebec City, Rapport Final; Réalisé Pour le Compte du Ministère des Forêts, de la Faune et des Parcs, Gouvernement du Quebec: Quebec City, QC, Canada; Centre D'études Nordiques, Université Laval: Quebec City, QC, Canada, 2018; p. 61.

32. SIGÉOM. Surface Deposits Map. Système D'information Géominière du Quebec. 2020. Available online: https://sigeom.mines.gouv.qc.ca/signet/classes/I1108_afchCarteIntr (accessed on 3 June 2021).
33. Government of CanadaLakes, Rivers and Glaciers in Canada—CanVec Series—Hydrographic Features. Available online: https://open.canada.ca/data/en/dataset/9d96e8c9-22fe-4ad2-b5e8-94a6991b744b (accessed on 15 May 2019).
34. Foretouverte. *Cartographie écologique de la VÉGÉTATION du NORD QUÉBÉCOIS*; Ministère des Forêts, de la Faune et des Parcs (MFFP): Quebec City, QC, Canada, 2018. Available online: https://www.foretouverte.gouv.qc.ca/ (accessed on 10 June 2021).
35. Lemieux, J.-M.; Fortier, R.; Talbot-Poulin, M.-C.; Molson, J.; Therrien, R.; Ouellet, M.; Banville, D.; Cochand, M.; Murray, R. Groundwater occurrence in cold environments: Examples from Nunavik, Canada. *Appl. Hydrogeol.* **2016**, *24*, 1497–1513. [CrossRef]
36. Philipp, M.; Dietz, A.; Buchelt, S.; Kuenzer, C. Trends in Satellite Earth Observation for Permafrost Related Analyses—A Review. *Remote Sens.* **2021**, *13*, 1217. [CrossRef]
37. Allard, M.; Lemay, M.; Barrette, C.; L'Hérault, E.; Sarrazin, D. Permafrost and climate change in Nunavik and Nunatsiavut: Importance for municipal and transportation Contributing authors. In *Nunavik and Nunatsiavut: From Science to Policy. An Integrated Regional Impact Study (IRIS) of Climate Change and Modernization*; Michel Allard, M.L., Ed.; ArcticNet Inc.: Quebec City, QC, Canada, 2012; Chapter 6; pp. 171–197.
38. Ulrich, M.; Matthes, H.; Schirrmeister, L.; Schütze, J.; Park, H.; Iijima, Y.; Fedorov, A.N. Differences in behavior and distribution of permafrost-related lakes in C entral Y akutia and their response to climatic drivers. *Water Resour. Res.* **2017**, *53*, 1167–1188. [CrossRef]
39. Duguay, C.R.; Zhang, T.; Leverington, D.W.; Romanovsky, V.E. Satellite Remote Sensing of Permafrost and Seasonally Frozen Ground. *Geophys. Monogr. Ser.* **2013**, *163*, 91–118. [CrossRef]
40. Arp, C.D.; Whitman, M.S.; Jones, B.M.; Grosse, G.; Gaglioti, B.V.; Heim, K.C. Distribution and biophysical processes of beaded streams in Arctic permafrost landscapes. *Biogeosciences* **2015**, *12*, 29–47. [CrossRef]
41. Owuor, S.O.; Butterbach-Bahl, K.; Guzha, A.C.; Rufino, M.C.; Pelster, D.; Diaz-Pines, E.; Breuer, L. Groundwater recharge rates and surface runoff response to land use and land cover changes in semi-arid environments. *Ecol. Process.* **2016**, *5*, 16. [CrossRef]
42. Gerlach, M.E.; Rains, K.C.; Guerrón-Orejuela, E.J.; Kleindl, W.J.; Downs, J.; Landry, S.M.; Rains, M.C. Using Remote Sensing and Machine Learning to Locate Groundwater Discharge to Salmon-Bearing Streams. *Remote Sens.* **2022**, *14*, 63. [CrossRef]
43. Belknap, W.; Naiman, R. A GIS and TIR procedure to detect and map wall-base channels in Western Washington. *J. Environ. Manag.* **1998**, *52*, 147–160. [CrossRef]
44. Ebersole, J.L.; Wigington, P.J.; Leibowitz, S.G.; Comeleo, R.L.; Van Sickle, J. Predicting the occurrence of cold-water patches at intermittent and ephemeral tributary confluences with warm rivers. *Freshw. Sci.* **2015**, *34*, 111–124. [CrossRef]
45. Peterson, N.P.; Reid, L.M. Wall-base channels: Their evolution, distribution, and use by juvenile coho salmon in the Clearwater River, Washington. In Proceedings of the Olympic Wild Fish Conference, Port Angeles, WA, USA, 23–25 March 1983; pp. 215–225.
46. Liu, S.; Feng, Y. *Airborne GPR: Advances and Numerical Simulation College of Geo-Exploration Sci & Tech*; Jilin University: Changchun, China; The third Railway Survey and Design Institute Group Corporation: Tianjin, China, 2011; pp. 3397–3400.
47. Campbell, S.; Affleck, R.T.; Sinclair, S. Ground-penetrating radar studies of permafrost, periglacial, and near-surface geology at McMurdo Station, Antarctica. *Cold Reg. Sci. Technol.* **2018**, *148*, 38–49. [CrossRef]